LIP-STUDENTS-22-19

Geo-neutrinos

Margarida Ferreira[1,a]

[1] *FCTUC, Coimbra, Portugal*

Project supervisor: Sofia Andringa

November 13, 2022

Abstract. Geo-neutrinos are an important probe to study inaccessible parts of the earth's interior. This paper provides a brief study on how an uranium mine could interfere in the interpretation of the results from geo-neutrinos detectors, with parameters similars to SNO+ detector. SNO+ is a liquid scintillator-base experiment that contains approximately 10^{32} free protons, and is very sensitive to electron anti-neutrinos. In this project we try to calculate if these effects could be considered negligible. Simulations were made with inputs from Cigar Lake mine data. Results showed us that for close distances (smaller than 30 km) from the detector to the mine, uranium energy spectrum gets significant higher than the expected one. The same does not happen for far distances, even when the electron neutrino survival probability is high. Thus, for an accurate prediction of the local geo-neutrino signal from the crust, the presence of uranium mines must not be neglected.

Keywords: SNOLAB, SNO+, Inverse Beta Decay, Uranium, Mine

1 Introduction

1.1 SNO+ Detector

SNO+ is located at SNOLAB (Sudbury Neutrino Observatory Lab) facility, which is an underground science research laboratory, specializing in astroparticle physics.

The primary focus of SNOLAB is neutrino and dark matter physics, it is the cleanest lab in the world. It could be said that SNO+ is the successor of the SNO (Sudbury Neutrino Observatory) experiment, as it reuses the equipment of the SNO detector, replacing the heavy water from SNO with liquid scintillator.

SNO+ is a large liquid scintillator detector for studying neutrinoless double beta decay. In addition to this, SNO+ has other purposes, which includes the study of geo antineutrinos from radioactive decays in the Earth. The detector is located 2 km below the surface in Vale's Creighton nickel mine near Sudbury, Ontario, Canada. The deep underground location of SNO+ makes it less sensitive to cosmic rays background, allowing physics searches on challenging subjects.

The center of the SNO+ detector is an acrylic sphere with a 12 meter diameter, filled with 780 tonnes of liquid scintillator, loaded with 1.3 tonnes of Te 130. Liquid scintillator is an organic liquid, less dense than water, that gives off light when charged particles pass through it, counting the resultant photon emissions. The scintillator used in the SNO+ experiment is mainly composed of Linear Alkyl Benzene (LAB), which is very transparent, has good light output and is chemical compatible with acrylic. Liquid scintillation counting is used numerous times for beta particle detection. The scintillator is contained within a spherical acrylic vessel (AV) of 5 cm thickness with 7.000 tonnes of purified water surrounded by nearly 9.400 Hamamatsu R1408 photomultiplier tubes (PMTs), which are very sensitive light detectors. Neutrinos from nuclear reactors, supernovas, the Sun, and from heat-producing elements decays, such as thorium and uranium, inside the Earth will interact and then be detected by the PMTs.

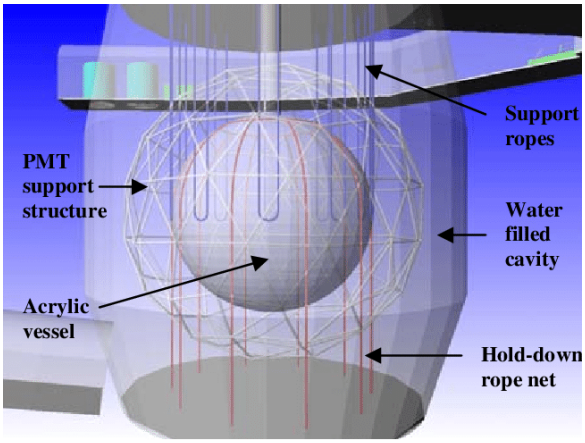

Figure 1. SNO+ Detector Structure

1.2 SNO+ Phases

The SNO+ operation consisted of three experimental phases, which each allows for the investigation of different physics topics. The detector components calibration and background measurements were made in the first phase, that started in 2016, known as the "Water-Phase". At this stage the detector was filled with ultra-pure water, allowing measurements of events occurring both inside and outside the acrylic vessel. The second is the "Pure Liquid Scintillated Phase", which has characterized the backgrounds of the scintillator. During this phase the detector was filled with scintillator at the top and water at the bottom. Reactor and geo antineutrinos, and supernova neutrinos could be measured. The final phase is "The Telurium Loaded Liquid Scintillator Phase". The aim is the search for neutrinoless double beta decay with Te 130.

[a] e-mail: margaridartf@gmail.com

1.3 Neutrino

Austrian physicist Wolfgang Pauli(1900-1958) postulated a particle in 1930 in order to preserve the principle of energy, and the angular and linear momenta of particles emitted in beta decay. It was Enrico Fermi (1901-1954) who named the particle "neutrino, the little neutral one", because it was much smaller than the neutron. In 1956 Frederick Reines (1918-1998) and Clyde Cowan (1919-1974), in work with other investigators, made the first discovery of the neutrino particle.

Neutrinos are uncharged particles, that interact very weakly with matter, making it difficult to detect. They only interact through the weak force and gravity. They are the lightest of all the subatomic particles that have mass. Geoneutrinos are neutrinos or antineutrinos (the inverse particle of neutrinos) that are emitted in decays chains occurring in the earth. This work depends only on beta minus decays, that emit antineutrinos, but not neutrinos. Because of weak interaction with normal matter, neutrinos travel in a straight line, at a velocity close to light's as a mixture of three different flavours:

- electron neutrino (ν_e);
- muon neutrino (ν_μ);
- tau neutrino (ν_τ).

They are produced in one state, and could be detected in a different state, therefore they oscillate. We can only see them when they interact, producing one particular flavour. Owing to the fact that they oscillate, we can say that they experience time, and therefore have mass. However only differences between masses can be measured by interferometry. Each flavour is represented by a quantum state $|\nu_X\rangle$ which is a linear combination of three neutrino mass states $|m_i>$, i.e. the three flavour eigenstates are a combination of three mass eigenstates, which are eigenstates of the free particle's hamiltonian. Only electron geo neutrinos can be produced by radioactive decays, due to the fact that the masses of the muon and tau (106 and 1,777 MeV, respectively), are much higher than the decay energy. We used the normal mass ordering (NO), instead of the inverse one (IO), $m_1 < m_2 < m_3$. In this project, we worked with the three-flavour neutrino survival probability, although we started by using the effective two-flavour approximation, it ended up not being a reliable estimation. The actual survival probability is the product of the survival probability and the uranium energy spectrum.

The probability of any neutrino flavour be detected in the same flavour (assuming CPT invariance) is given by:

$$P(\nu_e \to \nu_e) = 1 - \Big[cos^4(\theta_{13})sin^2(2\theta_{12})sin^2(1,27\Delta m^2_{21}\tfrac{L}{E}) + \\ + cos^2(\theta_{12})sin^2(2\theta_{13})sin^2(1,27\Delta m^2_{31}\tfrac{L}{E}) + \\ + sin^2(\theta_{12})sin^2(2\theta_{13})sin^2(1,27\Delta m^2_{32}\tfrac{L}{E})\Big], \quad (1)$$

where θ_{12} and θ_{13} are the solar and reactor neutrino mixing angles, respectively, $\Delta m^2{}_{ji}$ is the neutrino mass-squared difference in eV^2, L is the distance in meters, and E is the antineutrino energy in MeV. These are the values used: $\theta_{13} = 0.14959\ rad$, $\theta_{12} = 0.584\ rad$, $\Delta m^2_{21} = 7.42\times10^{-5} eV^2$, $\Delta m^2_{31} = 2.5140\times10^{-3} eV^2$, and $\Delta m^2_{32} = 2.4398\times10^{-3} eV^2$. We are more likely to detect certain flavours depending on the neutrinos energy and how far it has travelled. As we can observe on the graphics 2 and 3 the probability of detecting any neutrino flavour goes up and down as the neutrino travels.

However in most cases, in particular ours, an average survival probability is more likely to be approximated, since it is necessary to integrate the whole crust of the earth:

$$\langle P_{ee}\rangle \simeq cos^4\theta_{13}\Big(1 - \tfrac{1}{2}sin^2 2\theta_{12}\Big) + sin^4\theta_{13} \quad (2)$$

On average, we have $\langle P_{ee}\rangle = 0.55\pm0.01$.

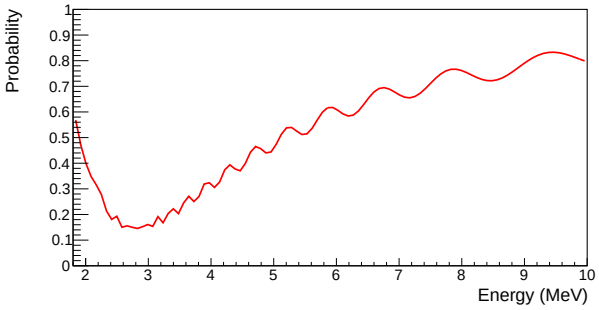

Figure 2. Survival probability of any neutrino flavour be detected in the same flavour, with three masses, at a distance of 46.5 km.

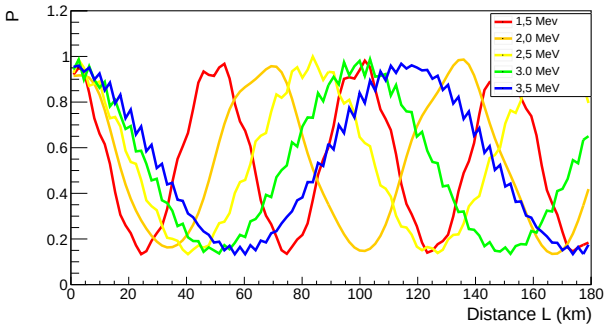

Figure 3. Antineutrino Survival probability, with three masses, and different energies.

1.4 Inverse beta Decay (IBD) : $\overline{\nu_e} + p \to n + e^+$

This interaction between an antineutrino and a proton is very much like the beta decay (in which the neutron transforms into a proton, an electron and an antineutrino), but inverted: it is the antineutrino that interacts with a proton (typically a Hydrogen nucleus) creating a neutron and a positron. Note that at low energy this is only possible for electron antineutrinos, as there is no energy to create a muon or a tau.

It has a very clear signature: the positron will loose its kinetic energy and then annihilate with an electron in matter, producing two 0.511 MeV gamma rays, followed by the delayed signal of a 2.2 MeV gamma ray from neutron capture by a proton, with a typical time of ~200 ms. This nuclear reaction is detected in the liquid scintillator by PMTs.

However we can only detect electron antineutrinos emitted by ^{232}Th and ^{238}U decay chains, because they have energies above 1.8 MeV (threshold energy). A minimum energy is necessary in order to produce a positron and a neutron in the beta minus decay. This energy is calculated through the expression (using the neutron, proton, and electron masses):

$$E_{\bar{\nu}} = (m_n - m_p + m_e) = 1.8 \text{ MeV} \tag{3}$$

Antineutrinos produced by the ^{40}K decay chains are not visible to the detector, as they have an energy lower than 1.8 MeV. ^{232}Th and ^{238}U have very long decay chains, with half-lives close to earth's age, which allow us to study data about our planet's interior including the global flux of energy:

$$\begin{aligned} ^{232}\text{Th} &\rightarrow {}^{208}\text{Pb} + 6\,{}^{4}\text{He} + 4e^- + 4\overline{\nu_e} + 42.7 \text{ [Mev]}, \\ ^{238}\text{U} &\rightarrow {}^{206}\text{Pb} + 8\,{}^{4}\text{He} + 8e^- + 6\overline{\nu_e} + 51.7 \text{ [Mev]}. \end{aligned} \tag{4}$$

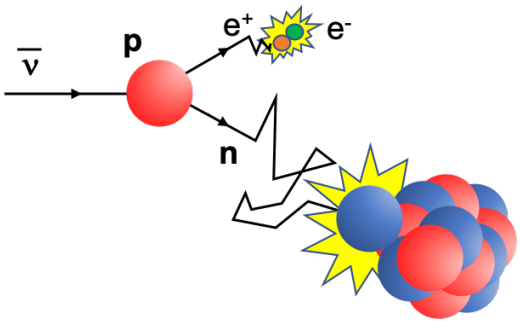

Figure 4. Inverse Beta Decay Signature. In this particular figure the reaction is not on free hydrogen nucleus.

1.5 Objectives

The aim of this project is to understand if the presence of an uranium mine close to a geo-neutrino detector can make any difference in the observed data. This study provides an useful information for more sensitive measurements able to separate geo-neutrinos from anti-neutrinos produced in other processes. For that purpose, we worked with the energy spectrum on Geoneutrinos[1], using SNO+ location. Additionally, we simulated data using Cigar Lake uranium mine, located in Canada. For data analysis, we used the framework ROOT.

2 Data Simulation

2.1 Geoneutrinos Energy Spectrum

In order to make a realistic simulation, we used the real geoneutrino energy spectrum data from [1], with SNOLAB latitude and longitude (46.47°N, 81.17°W). The energy spectrum of the antineutrino interaction rate in units of Terrestrial Neutrino Units (TNU) per keV against MeV is represented in figure 5. 1 TNU corresponds to 1 antineutrino event (1 IBD) measured over a 1 year by a detector containing 10^{32} free protons target. The graph has tree components: uranium geoneutrinos, thorium geoneutrinos, and total. The total includes reactor cores, a closest core, a user-defined core, and U and Th geoneutinos.

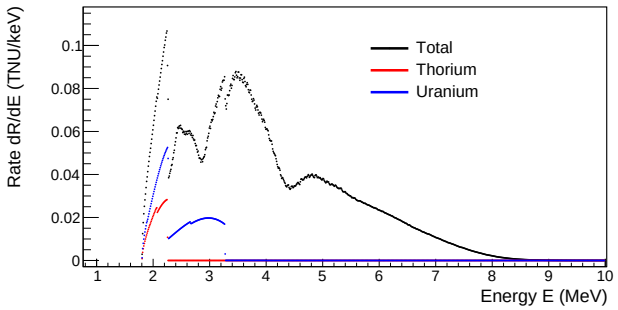

Figure 5. Energy spectrum of the antineutrino interaction rate.

2.2 Uranium Mine

Cigar Lake mine is an underground uranium mine located in the uranium-rich Athabasca Basin of northern Saskatchewan province, Canada. As it is one of the largest world's uranium deposits, it was ideal for our simulations in order to hypothesize significant results.

First of all, we had to take in account the quantity of kilograms of uranium available in the mine. According to the technical report[2], Cigar Lake has 75 kilotonnes of U^3O^8, which corresponds to 59.63×10^6 kg of ^{238}U (its natural abundance is 99,28%). We know, as it is described in literature [3], that 74 antineutrinos are emitted per kg per μs.

Secondly, we calculated the best distance that would maximize the antineutrino survival probability, i.e. P($\nu_e \rightarrow \nu_e$) has to be equal to 1. Besides zero, which is impossible because the detector is not in the same exact place as the mine, the first maximum of the function is 69 km if the energy is 2 MeV, and 97 km if the energy is 3 MeV.

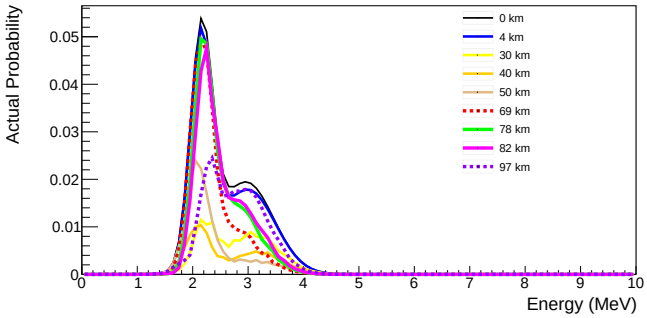

Figure 6. Actual Survival probability for different distances. The uranium energy spectrum was normalized by fitting two gaussians, as mentioned in subsection 2.3.

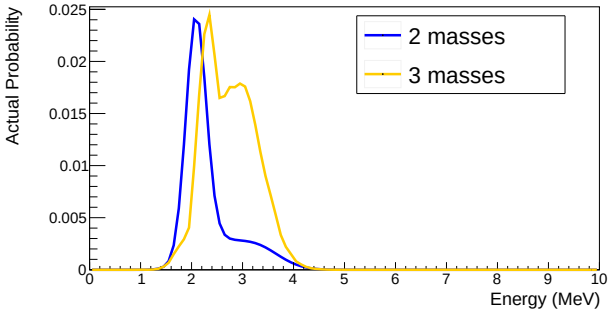

Figure 7. Actual Survival probability for antineutrinos emitted from uranium decay chains with two and three flavours, at a distance of 46.5 km.

After plotting the product of the survival probability with the uranium spectrum for different distances, and calculating their integral, we realized, by trial and error, that both 78 and 82 km maximize the function. From that moment, we decided to use 78 km as the best distance. Although 82 km wouldn't make any difference for the survival probability, the antineutrino flux would be smaller. In spite of that, the factor $P_{ee}(r)$ must also be considered.

As shown through the graphics in figure 6, for small distances, close to 0 km, there hasn't been enough time for antineutrinos to oscillate, so the survival probability for electron antineutrino is higher in comparison to others. Because the function is given by sinusoidal parameters, the same happens for far distances, such as 82 km. At a distance of 40 km, antineutrinos had oscillated thus, their interaction probability is lower. Looking back at figure 2, particularly at 2.0 and 3.0 MeV energies functions, we can confirm the intervals of distance where the probability is higher, and verify that these intervals start to be more and more far apart. Besides, a higher energy gives a bigger wavelength to the particle, making it oscillate slower.

The quantity of geo-neutrinos arriving to the detector decreases as the distance squared increases. The order of magnitude for the IBD cross section σ is $10^{-42} cm^2$. Therefore, most antineutrinos do not interact with the target, even whose energy is bigger than 1.8 MeV. Spectrum in figure 5 has already in consideration that parameter, as well as the average survival probability, $\langle P_{ee} \rangle$.

Figure 7 indicate us the difference between the survival probability function for antineutrinos emitted from uranium decay chains, with two and three masses, in the blue and yellow graphics, respectively.

2.3 Comparing the Mine Energy Spectrum

With the focus on knowing the influence of geo-neutrinos from a mine, we decided to calculate the fraction between the energy spectrum of antineutrinos emitted from uranium beta decays from the mine and the earth, in two distinct ways (cross-checking), so the result could be more reliable. Since we will discuss different outputs for different distances, the result will be given as a function of the distance in km. Even though, the survival probability appears in these calculations, we assumed the approximation in equation2, and we only worked with it later on when using equation 8.

The first way to do this comparison is by multiplying the volume of the mine with the density of uranium in the mine and divide it by the squared distance of the mine to the detector, and then do the volume integral of the uranium's density on the crust multiplied by the squared distance from any place on earth's crust to the detector (d).The integration is done over the whole volume of the crust, given that geoneutrinos flux is typically dominated by the crustal contribution. Additionally, we have to multiply the common terms. Finally, calculate the fraction between the two previously mentioned terms:

$$\frac{D_{mine}}{D_{crust}} = \frac{\frac{V_m \times \rho_m}{r^2}}{\oint_{crust} \rho_c / d^2 \, dV} \times \frac{r_\nu(E_\nu).P_{ee}(E_\nu, d).\sigma(E_{\nu_e}).p.t}{r_\nu(E_\nu).P_{ee}(E_\nu, d).\sigma(E_{\nu_e}).p.t} \quad (5)$$

These are the values used: $V_m = 3{\times}10^6$ m^3; $\rho_m = 20\ kg/m^3$; $\oint_{crust} 1/d^2\, dV = 1.57{\times}10^3$ m; $\rho_c = 2.25{\times}10^{-3} kg/m^3$. In the common term we applied $r_\nu(E_\nu) = 74\ \overline{\nu}/kg/\mu$s and $\sigma(E_{\nu_e}) = 10^{-42}\ cm^2$. Although, they depend on the energy and antineutrinos's are not all equal to the threshold energy of IBD, we can consider them a strong approximation. Besides that we also assumed $P_{ee}(E_\nu, d)$ equal to 0.55, so the numerator and denominator could cut. Finally, we multiplied the amount of protons in the SNO+ detector, p=10^{32} and the total of seconds found in a year, t=$3.15{\times}10^7$ s.

The fraction gave us a result of $\frac{16.99}{r^2} cm^{-2}$.

The second method involved the determination of the TNU detected from the mine R_{mine}, and then the comparison between the ones from the rest of the planet R_{crust}:

$$\mathrm{R}_{mine} = \mathrm{N}_{^{238}U}.r_\nu(E_\nu).P_{ee}(E_\nu, d).\sigma(E_{\nu_e}).p.t/r^2 \tag{6}$$

$N_{^{238}U}$ is the quantity of ^{238}U present in the mine, 59.63×10^6 kg, multiplying by $r_\nu(E_\nu)$ we have the number of antineutrinos emitted per second. Next it was necessary to multiply it by the cross section and by p together with t to get the result in TNU. Geoneutrinos provided us the number of TNU from all the other ^{238}U on crust, 25.8 TNU. Having in mind that the natural abundance of uranium on earth is ^{238}U isotope, we are not considering ^{235}U. After the division, we get $\frac{R_{mine}}{R_{crust}} = \frac{53.60}{r^2}\ cm^{-2}$.

Lastly, we dived the two fractions (the second one by the first) for a better comparison, which gave us a factor of 3.15. Due to the approximations used, it was expected to get a result different from 1. Nonetheless, these two results are in the same base unit which is a good indicator that we are using the correct forms.

Normalization

Since we already had the uranium energy spectrum, it was necessary to normalize it for the uranium mine. The function that represents the uranium energy spectrum could be described by the sum of two gaussian functions divided by a factor of 41 to be normalized as the uranium spectrum in figure 5, this value was chosen by overlapping the functions until they coincided. A normalized gaussian function is given by the expression:

$$g(x) = \frac{e^{-0,5(\frac{x-\mu}{\sigma})^2}}{\sigma\sqrt{2\pi}}, \tag{7}$$

where the parameters μ and σ are the mean value and the standard deviation, respectively, in units of MeV. The first one $g_1(x)$, has a mean value of 2.16 and a sigma of 0.2, the other one $g_2(x)$, a mean value of 2.96 and a sigma of 0.5. These parameters were chosen by root, since it has an option to find out the equation that best describes a line of a function. Considering that function, we multiplied it by the fraction between TNU from the mine and the crust, and the fraction between the survival probabilities (the factor of the inverse squared distance has already be taken in account in equation 6).

$$\frac{g_1(x)+g_2(x)}{41} \times \frac{R_{mine}}{R_{crust}} \times \frac{P_{ee}(r)}{\langle P_{ee}(d)\rangle} \tag{8}$$

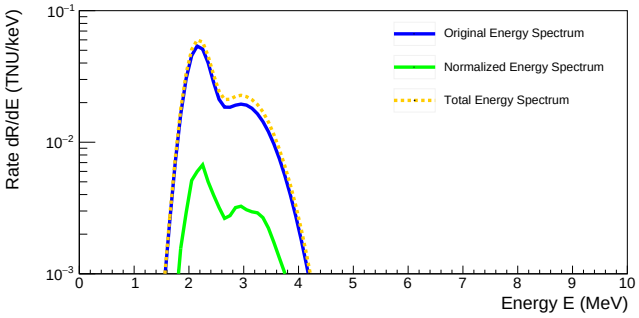

(a) r=20 km, $\frac{R_{mine}}{R_{crust}}$=0.134 and $\frac{P_{ee}(r)}{\langle P_{ee}(d)\rangle}$= 1.04.|

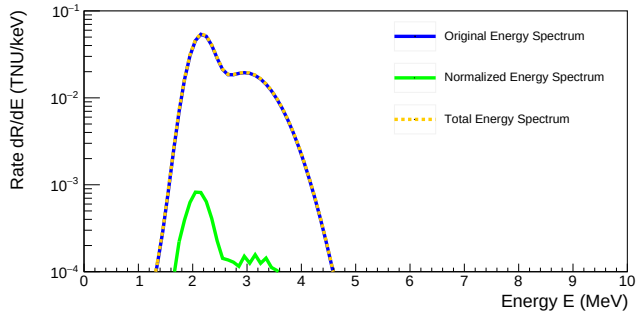

(b) r=46.5 km, $\frac{R_{mine}}{R_{crust}}$=0.0248 and $\frac{P_{ee}(r)}{\langle P_{ee}(d)\rangle}$=0.472.

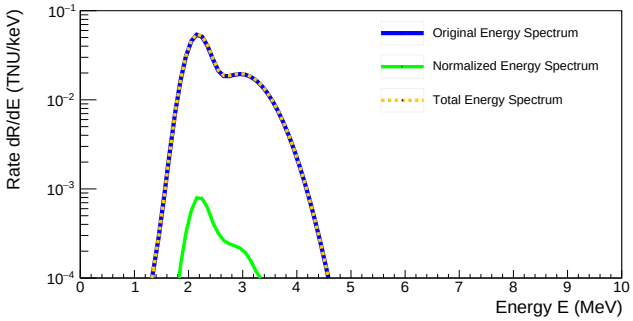

(c) r=78 km, $\frac{R_{mine}}{R_{crust}}$=0.00881 and $\frac{P_{ee}(r)}{\langle P_{ee}(d)\rangle}$=1.35.

Figure 8. Comparison of the original uranium spectrum with the normalized mine spectrum using a logarithmic scale, for different distances.

3 Results and Conclusions

	Energy Spectrum (TNU)		
Distance	Original	Normalized	Total
20.0 km	0.0476561	0.00663833	0.05429443
46.5 km	0.0476561	0.000557513	0.048213613
78.0 km	0.0476561	0.000564779	0.048220879

Table 1. Integral values of the energy spectrum functions given in TNU. Given the original integral values, we can multiply the fractions's values $\frac{R_{mine}}{R_{crust}}$ and $\frac{P_{ee}(r)}{\langle P_{ee}(d)\rangle}$ in figure 8 to obtain the normalized integral values.

When trying to obtain the normalized uranium spectrum to add it to the original one, we started with a close distance to the mine – 20 km, but not overly close as it could be unrealistic. Looking at the graphic 2.3, we see that the total energy spectrum highlights from the original one, the percentage of TNU detected from the uranium mine is considerable. Besides the detector being at a close distance, the electron antineutrinos had not have enough time to oscillate, so the survival probability is higher.

Graphics from images 2.3 and 2.3 are pretty similar, even tough having separate distances. In both cases, we can not see the total uranium spectrum line standing out as the normalized spectrum is much smaller than the original one.

When using a distance of 46.5 km, the electron antineutrinos have a lower survival probability since most of them had already oscillated. Although 78 km is a farther distance than 46.5 km, antineutrinos have a higher survival probability, because some of them had more time to be detected again as an electron antineutrino. When calculating the integral values of the total energy spectrum, as shown in table 1, we realize that there are slightly more events detect at a distance of 78 km than 46.5 km.

The results demonstrate that for distances smaller than 30 km, the percentage of detected antineutrinos emitted from the mine are very significant. Therefore, data from a mine with Cigar Lake‘s dimensions has to be taken in consideration in order to study reliable models. Furthermore, these results indicate us that it would be possible to discover an unknown mine close to the detector, since the geo-neutrinos energy spectrum is significant higher than what would be expected.

On the other side, for longer distances, the existence of unknown mines on the earth‘s crust would not have an extreme impact on the energy spectrum, which in some research works could be seen as a positive aspect, because it allows investigators to neglect it.

Even though the difference between the original and total uranium spectrum is not extremely emphasize, it should not be neglected if, for instance, there is an error bigger than what it was expected by the presence of an uranium mine.

These simulations were made using SNO^+ parameters, such as the number of free protons. However, there are detectors with a bigger number of protons which means that in those cases, the influence of unknown mines at a far distance could have a much significant influence, since more events would be detected. At the same time, more events from the rest of the crust would also be detected, making the fraction between them similar. Nevertheless, at a bigger scale the total uranium spectrum could stand out from the original spectrum and therefore, have an important effect on the data analysis.

A more general overview on the uranium mines effects would be of interest to further geo-neutrinos researches, since these effects could differ considerable, depending on aspects such as the distance to the mine, its density, and the amount of protons and years used in the detection.

Acknowledgements

I would like to thank LIP for providing this internships program for students, as well as my supervisor Sofia Andringa for all the support, availability and guidance. I also want to express a word of gratitude to my family, and my colleagues Yanhan Zhou and André Morais. This was an enriching opportunity, that gave me a closer look at the world of research and a great learning experience.

References

[1] A. Barna, S. Dye, *Web application for modeling global antineutrinos*, https://geoneutrinos.org/ (2015), [Online]

[2] C.S. Bishop, A.G. Mainville, L.D. Yesnik, *Cigar Lake Operation, Northern Saskatchewan, Canada*, https://s3-us-west-2.amazonaws.com/assets-us-west-2/technical-report/cameco-2016-cigar-lake-technical-report.pdf (2016), [Online]

[3] H. Minakata, Report YACHAY-PUB-17-02-PN (2017)

[4] G. Fiorentini, M. Lissia, F. Mantovani, R. Vannucci, *Geo-neutrinos: A new probe of Earth's interior*, https://www.sciencedirect.com/science/article/abs/pii/S0012821X05004103 (2005), [Online]

[5] P. Vogel, J.F. Beacom, *The angular distribution of the reaction* $\overline{\nu_e} + p \rightarrow e^+ + n$, https://arxiv.org/pdf/hep-ph/9903554v1.pdf (1999), [Online]